On the Interior Resonance Problem When Applying a Hybrid FEM/MoM Approach to Model Printed Circuit Boards

Yun Ji, *Member, IEEE,* and Todd H. Hubing, *Senior Member, IEEE*

***Abstract*—A hybrid finite element method/method of moments (FEM/MoM) technique is used to analyze a printed circuit board power bus structure where the source and observation points are in the near field. The FEM is used to model the lossy region between the planes of the board including the source. The MoM is used to model the region outside the planes and provide a radiation boundary condition to terminate the FEM mesh. Numerical results for a bridged power bus structure are compared with measurements. A nonphysical interior resonance of the electric field integral equation is observed. The problem can be avoided by using a hybrid technique based on a combined field integral equation.**

***Index Terms*—CFIE, EFIE, FE-BE, FE-MM, hybrid FEM/MoM, interior resonance, internal resonance, power bus structures.**

I. Introduction

THE HYBRID finite element method/method of moments (FEM/MoM) method, which is also referred to as FE-BE, FE-MM, FE-BI, or FEM/BEM in the literature, is often used to model electromagnetic scattering problems involving three-dimensional (3-D) inhomogeneous objects [1]–[5]. This method divides an electromagnetic problem into interior and exterior equivalent problems. The interior equivalent problem is modeled using the FEM. The exterior equivalent problem is represented by a surface integral equation, e.g., the electric-, magnetic- or combined-field integral equation (EFIE, MFIE or CFIE), and solved using the MoM. The FEM and MoM are coupled by enforcing the continuity of tangential fields on the boundary that separates the interior and exterior problems. The Sommerfeld radiation condition is built into the integral equation by using the scalar free-space Green's function. The coupled FEM and MoM equations provide a unique and exact solution to Maxwell's equations in both the interior and exterior regions.

The hybrid FEM/MoM has also been used to calculate radiation and circuit parameters of printed circuit board (PCB) structures in order to model electromagnetic interference (EMI) and signal integrity (SI) problems [6]–[8]. PCB structures usually contain metal and thin, lossy dielectrics that present significant challenges to numerical methods. Using the hybrid FEM/MoM, the details of the PCB are modeled by FEM without requiring extensive computer resources, and MoM is used to provide an accurate radiation boundary condition to terminate the FEM mesh. FEM can inherently model problems involving lossy inhomogeneous media, which are a significant challenge to pure MoM approaches.

FEM techniques that employ absorbing boundary conditions (ABCs) may not be efficient when modeling PCB structures that are thin in one direction. Using a hybrid FEM/MoM technique, the MoM boundary can be located very close to the PCB as long as the exterior equivalent problem is homogenous. Therefore, hybrid FEM/MoM techniques tend to be much more efficient for modeling PCB structures than pure FEM or MoM approaches. In addition, an FEM/MoM approach is well suited for modeling a PCB with shields or attached cables since large metallic objects can be modeled more efficiently using MoM.

Theoretically, the EFIE and MFIE do not have unique solutions at discrete frequencies corresponding to the interior resonances of closed surface geometries [9]–[12]. Numerical techniques employing the EFIE or MFIE may break down near these frequencies. This is called the *interior resonance* problem or the *internal resonance* problem. The frequencies where the EFIE and MFIE fail are referred to as *interior resonance frequencies*. The interior resonance problem has been investigated for cases where the EFIE and MFIE are applied to model electromagnetic scattering from PEC, homogenous and inhomogeneous objects [9]–[12]. One remedy is to adopt the CFIE [9]–[12]. In scattering problems, sources are usually incident plane waves modeled using MoM, and the results of interest are the calculated radar cross section (RCS). Scattering problems are generally much less sensitive to modeling or discretization errors than problems where the source and/or observation points are in the near field. For the circuit board problems investigated in this paper, the sources are located inside the FEM volume, and the results of interest are near-field voltages and currents. The purpose of this study is to investigate how the interior resonance problem affects numerical solutions.

In this study, a hybrid FEM/MoM technique is applied to the analysis of two bridged planes on a printed circuit board. Section II briefly describes the hybrid FEM/MoM approach, how the source is modeled, and how the scattering parameters are calculated. Section III presents the false resonance problem observed in the numerical results and the proposed remedy. Section IV summarizes the contents of the paper.

Manuscript received September 29, 2000; revised October 1, 2002.

Y. Ji is with Intel Desktop Architecture Lab (DAL), Hillsboro, OR 97124-6497 USA (e-mail: steven.yun.ji@intel.com).

T. H. Hubing is with the Department of Electrical and Computer Engineering, University of Missouri-Rolla, Rolla, MO 65409 USA (e-mail: hubing@ ece.umr.edu).

Publisher Item Identifier S 0018-9375(02)04558-1.

II. The Hybrid FEM/MOM

A. Formulation

Fig. 1 shows an object illuminated by either an incident wave ($\mathbf{E}^{\text{inc}}$, $\mathbf{H}^{\text{inc}}$) or an impressed current source $\mathbf{J}^{\text{int}}$. The interior equivalent problem is modeled by using FEM to solve the weak form of the vector wave equation as follows [13]:

$$\int_V \left[\left(\frac{\nabla \times \mathbf{E}(\mathbf{r})}{j\omega\mu_0\mu_r} \right) \bullet (\nabla \times \mathbf{T}(\mathbf{r})) + j\omega\varepsilon_0\varepsilon_r \mathbf{E}(\mathbf{r}) \bullet \mathbf{T}(\mathbf{r}) \right] dV = \int_S (\hat{n} \times \mathbf{H}(\mathbf{r})) \bullet \mathbf{T}(\mathbf{r})\, dS - \int_V \mathbf{J}^{\text{int}}(\mathbf{r}) \bullet \mathbf{T}(\mathbf{r})\, dV \quad (1)$$

where S is the surface enclosing volume V; $\mathbf{T}(\mathbf{r})$ is the weighting (testing) function. The electric field can be approximated by using the vector tetrahedral element $\mathbf{w}(\mathbf{r})$ proposed by Barton and Cendes [14], [15, ch. 2]

$$\mathbf{E}(\mathbf{r}) \approx \sum_{k=1}^{M} (E_i)_k \, \mathbf{w}_k(\mathbf{r}) + \sum_{n=1}^{N} (E_s)_n \, \mathbf{w}_n(\mathbf{r}) \quad (2)$$

where $\{E_i\}$ and $\{E_s\}$ are sets of unknowns for the electric field within volume V and on surface S. M and N are the number of basis functions within volume V and on surface S, respectively. The tangential magnetic field can be expanded using the triangular patch element $\mathbf{f}(\mathbf{r})$ proposed in [16]

$$\hat{n} \times \mathbf{H}(\mathbf{r}) \approx \sum_{n=1}^{N} (J_s)_n \, \mathbf{f}_n(\mathbf{r}) \quad (3)$$

where $\{J_s\}$ is a set of unknowns for the equivalent electric current on surface S. A Galerkin method can be used to discretize (1) as follows:

$$\begin{bmatrix} A_{ii} & A_{is} \\ A_{si} & A_{ss} \end{bmatrix} \begin{bmatrix} E_i \\ E_s \end{bmatrix} = \begin{bmatrix} 0 & 0 \\ 0 & B_{ss} \end{bmatrix} \begin{bmatrix} 0 \\ J_s \end{bmatrix} + \begin{bmatrix} g_i \\ g_s \end{bmatrix} \quad (4)$$

where A_{ii}, A_{is}, A_{si}, A_{ss} and B_{ss} are sparse coefficient matrices; g_i and g_s are source terms.

The exterior equivalent problem can be represented by using the EFIE [17]

$$\frac{\mathbf{E}(\mathbf{r})}{2} = \mathbf{E}^{\text{inc}}(\mathbf{r}) + \int_S \begin{bmatrix} -\mathbf{M}(\mathbf{r}') \times \nabla' G_0(\mathbf{r}, \mathbf{r}') - jk_0\eta_0 \mathbf{J}(\mathbf{r}') G_0(\mathbf{r}, \mathbf{r}') \\ +j \dfrac{\eta_0}{k_0} \nabla' \bullet \mathbf{J}(\mathbf{r}') \nabla' G_0(\mathbf{r}, \mathbf{r}') \end{bmatrix} dS' \quad (5)$$

or the MFIE (the dual of the EFIE) [17]

$$\frac{\mathbf{H}(\mathbf{r})}{2} = \mathbf{H}^{\text{inc}}(\mathbf{r}) + \int_S \cdot \begin{bmatrix} \mathbf{J}(\mathbf{r}') \times \nabla' G_0(\mathbf{r}, \mathbf{r}') - j \dfrac{k_0}{\eta_0} \mathbf{M}(\mathbf{r}') G_0(\mathbf{r}, \mathbf{r}') \\ +j \dfrac{1}{k_0\eta_0} \nabla' \bullet \mathbf{M}(\mathbf{r}') \nabla' G_0(\mathbf{r}, \mathbf{r}') \end{bmatrix} dS' \quad (6)$$

where $\mathbf{r} \in S$, η_0 and k_0 are the intrinsic impedance and wavenumber in free space, respectively. $\mathbf{J}(\mathbf{r})$ and $\mathbf{M}(\mathbf{r})$ in (5) and (6) are the equivalent surface electric and magnetic currents as shown in Fig. 1, and are defined and approximated as follows:

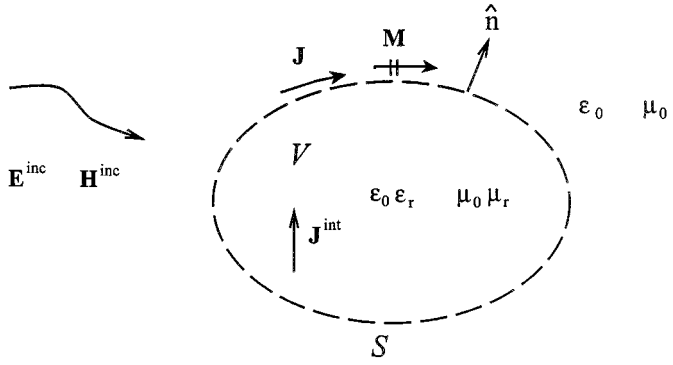

Fig. 1. An object illuminated by an incident wave or an impressed current source.

$$\mathbf{J}(\mathbf{r}) \equiv \hat{n} \times \mathbf{H}(\mathbf{r}) \approx \sum_{n=1}^{N} (J_s)_n \, \mathbf{f}_n(\mathbf{r}) \quad (7)$$

$$\mathbf{M}(\mathbf{r}) \equiv \mathbf{E}(\mathbf{r}) \times \hat{n} \approx \sum_{n=1}^{N} (E_s)_n \, \mathbf{f}_n(\mathbf{r}). \quad (8)$$

$\mathbf{E}(\mathbf{r})$ in (5) and $\mathbf{H}(\mathbf{r})$ in (6) are expanded on surface S using the tetrahedral basis function $\mathbf{w}(\mathbf{r})$ as follows:

$$\mathbf{E}(\mathbf{r}) \approx \sum_{n=1}^{N} (E_s)_n \, \mathbf{w}_n(\mathbf{r}), \qquad \mathbf{r} \in S \quad (9)$$

$$\mathbf{H}(\mathbf{r}) \approx -\sum_{n=1}^{N} (J_s)_n \, \mathbf{w}_n(\mathbf{r}), \qquad \mathbf{r} \in S. \quad (10)$$

If $\mathbf{f}_n(\mathbf{r})$, $n = 1 \cdots N$, are chosen to test (5), the formulation is called the TE formulation [11]. If $\hat{n} \times \mathbf{f}_n(\mathbf{r})$, $n = 1 \cdots N$, are chosen to test (5), the formulation is referred to as the NE formulation [11]. Similarly, the MFIE leads to the TH and NH formulations depending on the choice of testing functions [11].

The EFIE or MFIE may fail at some frequencies due to the existence of null space associated with the integral operators [9]–[12]. The CFIE is immune to this problem [9]–[12]. The CFIE is a linear combination of the EFIE and MFIE as follows:

$$\alpha LHS(\text{EFIE}) + (1-\alpha)\eta_0 LHS(\text{MFIE}) = \alpha RHS(\text{EFIE}) + (1-\alpha)\eta_0 RHS(\text{MFIE}) \quad (11)$$

where $LHS(\bullet)$ and $RHS(\bullet)$ denote the left-hand side and right-hand side of an equation, α is a real-value parameter in the range $0 < \alpha < 1$. The MFIE is multiplied by η_0 to scale the matrix coefficients. The optimal α parameter may be chosen to minimize the matrix condition number of the discretized (11) [18]. $\alpha = 0.5$ is used in this study to give equal weights to the EFIE and MFIE. Depending on how the EFIE and MFIE are tested, the CFIE has several variations [11]. The one used in this study is the TENH formulation, which uses $\mathbf{f}_n(\mathbf{r})$ to test the EFIE and $\hat{n} \times \mathbf{f}_n(\mathbf{r})$ to test the MFIE. The outgoing normal unit $\hat{n}$ in the NH formulation can be mathematically transferred to the MFIE in the test procedure. The TENH formulation is equivalent to the CFIE in [12].

After discretizing either the EFIE, MFIE or CFIE, the MoM matrix equation is in the following form:

$$[C][J_s] = [D][E_s] - [F^i] \tag{12}$$

where $[C]$ and $[D]$ are coefficient matrices, and $[F^i]$ is the excitation term. The FEM and MoM equations are coupled by enforcing the continuity of the tangential fields on the boundary. If the geometry contains a perfect electric conductor (PEC), the PEC boundary condition $\hat{n} \times \mathbf{E} = 0$ must be enforced in (2), (8) and (9).

Equations (4) and (12) then form a coupled and determined system. There are three different solution methods to solve the coupled matrix equation [19], [20]. The outward-looking solution method is employed in this study. It derives the RBC from (12)

$$J_s = C^{-1}DE_s - C^{-1}F^i. \tag{13}$$

Substituting (13) into (4) yields a determined matrix equation

$$\begin{bmatrix} A_{ii} & A_{is} \\ A_{si} & A_{ss} - B_{ss}C^{-1}D \end{bmatrix} \begin{bmatrix} E_i \\ E_s \end{bmatrix} = \begin{bmatrix} g_i \\ g_s - B_{ss}C^{-1}F^i \end{bmatrix}. \tag{14}$$

Iterative solvers can be used to solve (14). The preconditioning technique reported in [20] is used to improve the convergence rate and accuracy of the iterative solvers.

B. Source and Load

It is important to properly represent sources when the hybrid FEM/MoM method is used to model printed circuit power bus structures. On real boards, the power bus is normally driven by vias that penetrate the planes. When making measurements, these structures are often driven with a coaxial cable. The outer conductor of the cable is bonded to one metallic plane and the center conductor extends through to the opposite metallic plane. The reference plane of the measurement is normally calibrated to the cable opening, where the center conductor begins to extend beyond the outer conductor. Sources are normally modeled with the finite element portion of the hybrid FEM/MoM method. The probe and coaxial cable models are two widely used approaches for modeling the feed [5], [15, (ch. 7)].

The probe model represents the feed as a current filament along the center conductor of the coaxial cable. An impressed current source along the z-axis can be expressed as

$$\mathbf{J}^{\text{int}} = I_1\delta(x - x_f)\,\delta(y - y_f)\hat{\mathbf{z}} \tag{15}$$

where (x_f, y_f) specifies its position, I_1 denotes the electric current magnitude, and $\delta(x)$ is the Dirac delta function. Tetrahedral edges are chosen to coincide with the feed. The source term in (4) is then given by

$$\left[g^{\text{int}}\right]^e = I_1 l_1 \tag{16}$$

where l_1 is the edge length. The probe model is easy to implement and effective for modeling electrically-short feeding structures. This study uses the probe model for simplicity and satisfactory results are obtained.

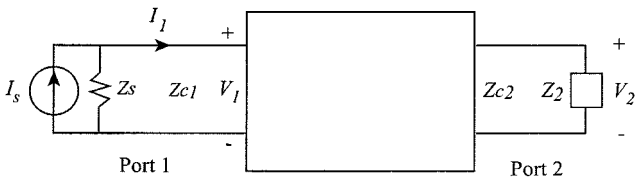

Fig. 2. The block diagram of a general two-port system.

C. The Scattering Parameters

The FEM/MoM method can be used to analyze the scattering parameters (S-parameters) of a two-port electromagnetic system as shown in Fig. 2. Z_{c1} and Z_{c2} are the characteristic impedances of Port 1 and Port 2, respectively. In this study, both Port 1 and Port 2 are 50-Ω systems, i.e., $Z_{c1} = Z_{c2} = 50\,\Omega$. The system is driven at Port 1 by a current source I_s with a source impedance of Z_s and terminated at Port 2 by a load Z_2. To obtain the scattering parameters, Z_s and Z_2 must be included in the formulation. The load impedance Z_2 can be modeled using a lossy dielectric post coinciding with a tetrahedron edge [21]. The post has a finite conductivity given by

$$\sigma = \frac{l}{Z_2 S} \tag{17}$$

where l is its length, and S is the cross sectional area. If the load is treated as a lumped element, its contribution to the finite element matrix is as follows:

$$[A]^e = \frac{(l)^2}{Z_2}. \tag{18}$$

The same approach can be use to model the source impedance Z_s.

The electric fields at the two ports, designated as E_1 and E_2, can be determined using the FEM/MoM solver. Then, the voltages at the two ports are given by

$$V_1 = E_1 d \qquad \text{and} \qquad V_2 = E_2 d \tag{19}$$

where d is the thickness of the board. V_1 is then decomposed into the incident voltage V_1^+ and the reflected voltage V_1^-. I_1 is decomposed into the incident current I_1^+ and the reflected current I_1^-. These parameters are related by transmission line theory as follows:

$$V_1^+ + V_1^- = V_1 \tag{20}$$

$$I_1^+ - I_1^- = I_1 = I_S - \frac{V_1}{Z_s} \tag{21}$$

$$I_1^+ = \frac{V_1^+}{Z_{c1}} \tag{22}$$

$$I_1^- = \frac{V_1^-}{Z_{c1}}. \tag{23}$$

Then, V_1^+ and V_1^- are given by

$$V_1^+ = \frac{Z_{c1}Z_s I_S + (Z_s - Z_{c1})\,V_1}{2Z_s} \tag{24}$$

$$V_1^- = \frac{(Z_s + Z_c)\,V_1 - Z_{c1}Z_s I_S}{2Z_s}. \tag{25}$$

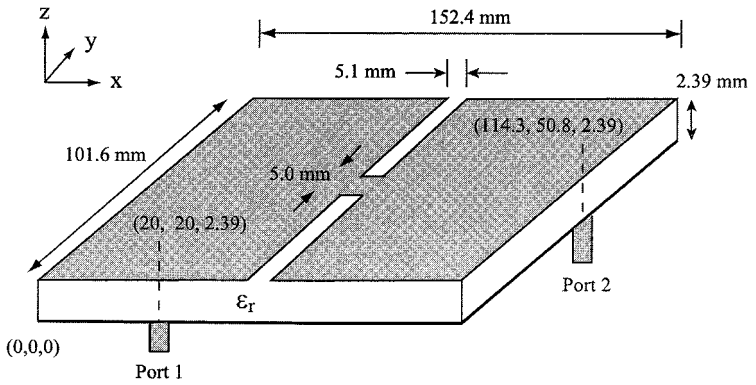

Fig. 3. The geometry of a bridged power bus structure.

In the case of $Z_s = Z_{c1}$, V_1^+ and V_1^- are given by

$$V_1^+ = \frac{Z_{c1} I_S}{2} \tag{26}$$

$$V_1^- = V_1 - \frac{Z_{c1} I_S}{2}. \tag{27}$$

To extract the S_{21} parameter, Port 2 must be matched, i.e., $Z_2 = Z_{c2}$, so that the following holds:

$$V_2^- = V_2 = E_2 d. \tag{28}$$

Then, S_{21} is given as follows:

$$S_{21} = \left. \frac{V_2^- \sqrt{Z_{c1}}}{V_1^+ \sqrt{Z_{c2}}} \right|_{\text{Port 2 matched}} = \frac{2E_2 d}{I_1 \sqrt{Z_{c1} Z_{c2}}} \quad \text{when } Z_s = Z_{c1}. \tag{29}$$

Similarly, other scattering parameters can be calculated.

III. The Interior Resonance Problem

Hybrid codes employing the EFIE (or MFIE) may exhibit significant errors at interior resonance frequencies. The interior resonance frequencies are the cavity-mode resonances of a PEC (or PMC, i.e., perfect magnetic conductor) structure formed by the MoM boundary and filled with the material in the exterior equivalent problem [11]. Mathematically, the integral operators of the EFIE (MFIE) have a null space, which means they have eigenvalues equal to zero. Consequently, there are no unique solutions to the EFIE (MFIE). Viewed another way, the MoM matrix [the C matrix in (12)] is the same matrix that represents a PEC (PMC) cavity, which does not have unique solutions at cavity-mode frequencies.

Bridged power bus structures are sometimes used in printed circuit board designs to prevent the noise generated by active devices from polluting other parts of the power bus and affecting sensitive (low noise margin) devices. Fig. 3 shows the geometry of a bridged power bus structure. The board is 152.4 mm $\times$ 101.6 mm $\times$ 2.39 mm. The bottom plane is copper and modeled as a PEC surface. The top plane is also copper except that there is a 5.1-mm wide gap located at the center along the y-axis and a 5.0-mm wide copper strip connecting the two patches. The material between the top and bottom planes has a dielectric constant that varies with frequency. The dielectric constant and loss tangent were determined using an experimental approach [22]. An approximate value for the dielectric constant as a function of frequency is given by

$$\varepsilon_r \approx \begin{cases} 4.6(1 - j0.01), & \text{frequency} < 400 \text{ MHz} \\ 4.4(1 - j0.015), & 400 \text{ MHz} < \text{frequency} < 1.0 \text{ GHz} \\ 4.2(1 - j0.02), & 1.0 \text{ GHz} < \text{frequency} < 2.0 \text{ GHz} . \end{cases}$$

An experimental board was built and two SMA connectors were attached to the locations designated in Fig. 3. A network analyzer was used to measure the magnitude of the transfer coefficient, $|S_{21}|$.

The first cavity mode supported by a PEC cavity is the TE_{110} mode. Therefore, the first interior resonance frequency for the bridged power bus structure is given by

$$f_{\text{interior}} = 150 \sqrt{\left(\frac{1}{0.1524}\right)^2 + \left(\frac{1}{0.1016}\right)^2} = 1774 \text{ MHz}. \tag{30}$$

Fig. 4 shows the $|S_{21}|$ results obtained using a hybrid FEM/MoM code near this interior resonance frequency at 1.0-MHz intervals. The numerical results obtained using the TE and TENH formulations in the MoM part are plotted and compared to the measured results. The same FEM formulation and mesh

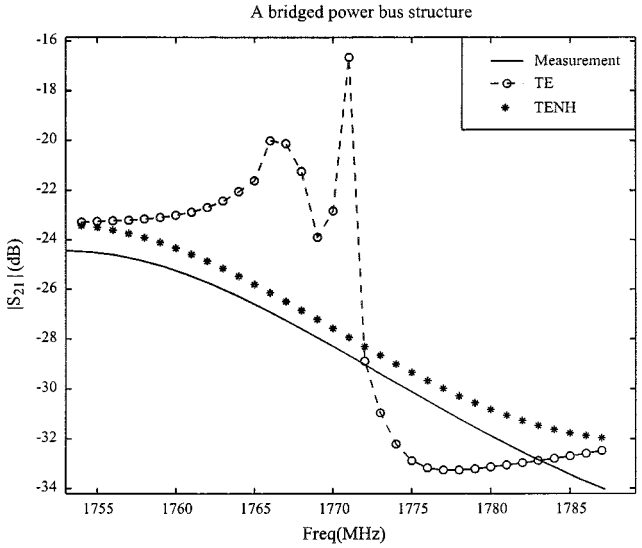

Fig. 4. The measured, TE and TENH $|S_{21}|$ results of the bridged power bus structure near the first interior resonance frequency.

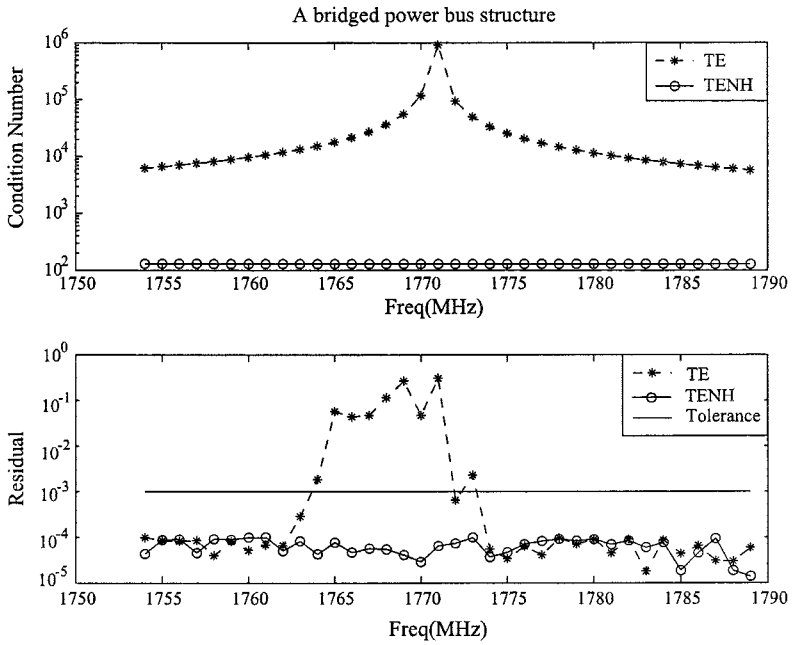

Fig. 5. The condition numbers of the MoM matrix and the residuals of iterative solutions near the first interior resonance frequency when modeling the bridged power bus structure.

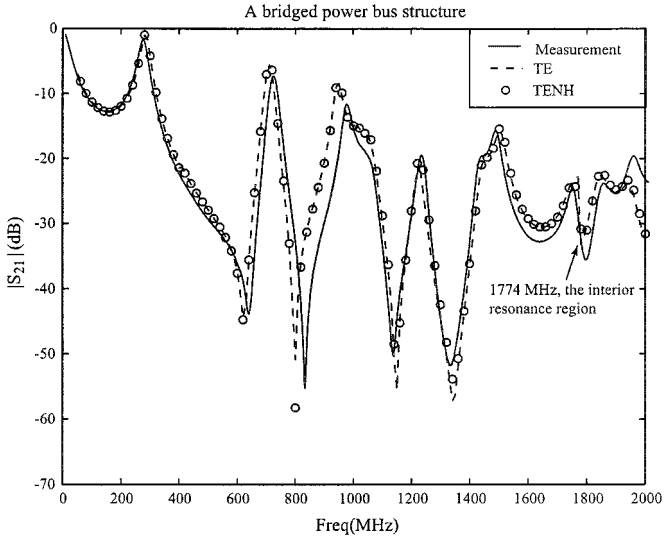

Fig. 6. The measured, TE and TENH $|S_{21}|$ results for the gapped power bus structure.

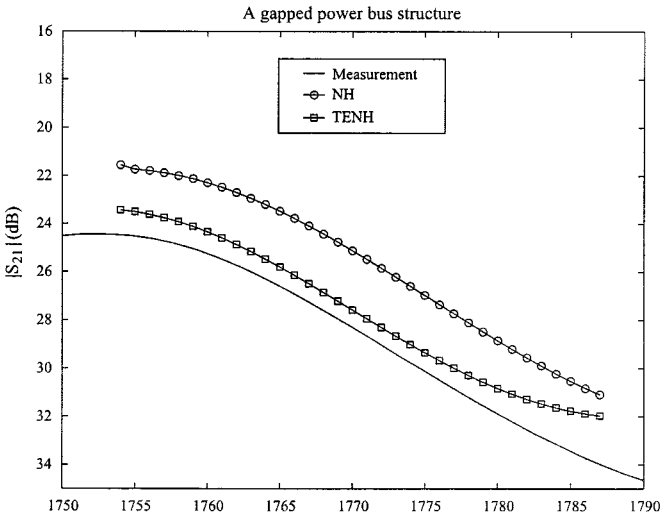

Fig. 7. The measured, NH and TENH $|S_{21}|$ results of the bridged power bus structure near the first interior resonance frequency.

were used in both numerical simulations. The TE results have an erroneous shape and a maximum error of 11 dB at 1771 MHz. The TENH formulation generates satisfactory results. The frequency range in which the TE formulation fails (i.e., results have more than the 3-dB error) is very narrow (about 1% of the calculated interior resonance frequency). This result agrees with that reported in [23] when MoM and FEM/MoM were used to analyze 3-D scattering problems. Fig. 5 shows the condition numbers of the MoM matrices and the residuals of the iterative solutions obtained using the complex bi-conjugate gradient stabilized (BiCGSTAB) method [24]. As expected, the condition numbers of the MoM matrices generated by the TE formulation peak in the vicinity of the interior resonance frequency. The iterative solver fails to generate satisfactory solutions because the radiation boundary condition provided by MoM is incorrect. Further numerical experiments showed the numerical errors could not be significantly reduced by increasing mesh density or choosing a different matrix solution method. The TENH formulation generates MoM matrices with much smaller condition numbers and the iterative solutions converge to the designated tolerance (10^{-3}).

The TE formulation only breaks down at the interior resonance frequencies [17]. Fig. 6 shows the measured, TE and TENH results for the bridged power bus structure at noninterior resonance frequencies at 20 MHz intervals. The two formulations generate almost identical results except small differences at dips of the $|S_{21}|$ curve. The numerical results agree with measurement very well at most frequency points. Near the $|S_{21}|$ peak at 980 MHz, there is a 30-MHz shift (3%) between the numerical and measured results. This may be caused by error in

the approximate value of the dielectric constant used in the numerical solution.

The interior resonance problem for MFIE formulations is well documented in the literature [9]–[12]. The PMC cavity formed by the MoM boundary supports a 110 mode at 1774 MHz. Fig. 7 compares measured, NH and TENH results near this frequency. The TENH formulation generates more accurate results than the NH formulation. The NH results have a 3-dB error in the interior resonance region, but do not have an erroneous shape as the EFIE results do. This is because the MFIE is generally superior to the EFIE when applied to closed surface geometries for reasons described in [12].

IV. Conclusion

An approach to model printed circuit board power bus structures using the hybrid FEM/MoM method has been presented. FEM is used to model the details of the structure and the feed. MoM is used to provide a radiation boundary condition to terminate the FEM mesh. The source and observation points are in the near field and the results of interest are current and voltage. The hybrid FEM/MoM employing the EFIE or MFIE in MoM is vulnerable to the interior resonance problem. The EFIE introduces more severe errors than the MFIE because the MFIE is better suited than the EFIE for modeling closed surface geometries. The CFIE formulation is shown to be free of the interior resonance problem. Good agreement between numerical results and measurements has been achieved.

Acknowledgment

The authors would like to thank the reviewers for their helpful suggestions and H. Wang, University of Missouri-Rolla, who generated some of the mesh files.

References

[1] X. Yuan, "Three dimensional electromagnetic scattering from inhomogeneous objects by the hybrid moment and finite element method," *IEEE Trans. Microwave Theory Tech.*, vol. 38, pp. 1053–1058, Aug. 1990.

[2] J.-M. Jin and J. L. Volakis, "Electromagnetic scattering by and transmission through a three-dimensional slot in a thick conducting plane," *IEEE Trans. Antennas Propagat.*, vol. 39, pp. 543–550, Apr. 1991.

[3] J. Angélini, C. Soize, and P. Soudais, "Hybrid numerical method for harmonic 3D Maxwell equations: Scattering by a mixed conducting and inhomogeneous anisotropic dielectric medium," *IEEE Trans. Antennas Propagat.*, vol. 41, pp. 66–76, Jan. 1993.

[4] G. E. Antilla and N. G. Alexopoulos, "Scattering from complex three-dimensional geometries by a curvilinear hybrid finite element-integral equation approach," *J. Opt. Soc. Amer. A*, vol. 11, no. 4, pp. 1445–1457, Apr. 1994.

[5] J. L. Volakis, T. Özdemir, and J. Gong, "Hybrid finite-element methodologies for antennas and scattering," *IEEE Trans. Antennas Propagat.*, vol. 45, pp. 493–507, Mar. 1997.

[6] A. Kost and H. Igarashi, "Different numerical methods for electromagnetic field computation with thin shielding sheets," in *Proc. IEEE Int. Symp. Electromagnetic Compatibility*, Austin, TX, Aug. 1997, pp. 248–253.

[7] Y. Ji and T. H. Hubing, "EMAP5: A 3D hybrid FEM/MoM code," *Appl. Computat. Electromagn. Soc. (ACES) J.*, vol. 15, no. 1, pp. 1–12, 2000.

[8] H. Wang, Y. Ji, T. H. Hubing, and J. L. Drewniak, "Radiation from right angle bends in microstrip traces," in *Proc. IEEE Int. Symp. Electromagnetic Compatibility*, Washington, DC, Aug. 2000, pp. 739–742.

[9] A. F. Peterson, "The interior resonance problem associated with surface integral equations of electromagnetics: Numerical consequences and a survey of remedies," *Electromagn.*, vol. 10, pp. 293–312, 1990.

[10] S. M. Rao and D. R. Wilton, "E-field, H-field, and combined field solution for arbitrarily shaped three-dimensional dielectric bodies," *Electromagn.*, vol. 10, no. 4, pp. 407–421, 1990.

[11] X. Q. Sheng, J.-M. Jin, J. Song, C.-C. Lu, and W. C. Chew, "On the formulation of hybrid finite-element and boundary-integral methods for 3-D scattering," *IEEE Trans. Antennas Propagat.*, vol. 46, pp. 303–311, Mar. 1998.

[12] D. S. Jones, *Methods in Electromagnetic Wave Propagation*, 2nd ed. New York: IEEE Press, 1994, ch. 6.

[13] P. P. Silvester and R. L. Ferrari, *Finite Elements for Electrical Engineers*, 3rd ed. New York: Cambridge Univ.Press, 1996, pp. 405–406.

[14] M. L. Barton and Z. J. Cendes, "New vector finite elements for three-dimensional magnetic field computation," *J. Appl. Phys.*, vol. 61, no. <AU: ISSUE NO:?>, pp. 3919–3921, 1987.

[15] J. L. Volakis, A. Chatterjee, and L. C. Kempel, *Finite Element Method for Electromagnetics*. New York: IEEE Press , 1998.

[16] S. M. Rao, D. R. Wilton, and A. W. Glisson, "Electromagnetic scattering by surfaces of arbitrary shape," *IEEE Trans. Antennas Propagat.*, vol. 30, pp. 409–418, May 1982.

[17] J. J. H. Wang, *Generalized Moment Methods in Electromagnetics*. New York: Wiley, 1990, ch. 6.

[18] L. M. Correia, "A comparison of integral equations with unique solution in the resonance region for scattering by conducting bodies," *IEEE Trans. Antennas Propagat.*, vol. 41, pp. 52–58, Jan. 1993.

[19] A. F. Peterson, S. L. Ray, and R. Mittra, *Computational Methods for Electromagnetics*. New York: IEEE Press, 1997, ch. 11.

[20] Y. Ji, H. Wang, and T. H. Hubing, "A novel preconditioning technique and comparison of three formulations for the hybrid FEM/MoM method," *Appl. Computat. Electromagn. Soc. (ACES) J.*, vol. 15, no. 2, pp. 103–114, 2000.

[21] J.-M. Jin, *The Finite Element Method in Electromagnetics*. New York: Wiley, 1993, pp. 324–325.

[22] C. Wang, "Determining dielectric constant and loss tangent in FR-4," Electromagnetic Compatibility Laboratory, Department of Electrical and Computer Engineering, University of Missouri-Rolla, Rolla, MO, TR00-1-41.

[23] M. S. Yeung, "Single integral equation for electromagnetic scattering by three-dimensional homogeneous dielectric objects," *IEEE Trans. Antennas Propagat.*, vol. 47, pp. 1615–1622, Oct. 1999.

[24] R. Barrett, M. Berry, T. F. Chan, F. Demmel, J. M. Donato, J. Dongarra, V. Eijkhout, R. Pozo, C. Romine, and H. Van der Vorst, *Templates for the Solution of Linear Systems: Building Blocks for Iterative Methods*. Philadelphia, PA: SIAM, 1994.

Yun Ji (S'97–M'02) received the B.S. degree in automatic control from Tsinghua University, Beijing, China in 1994, and M.S. and Ph.D. degrees in electrical engineering from the University of Missouri-Rolla,in 1997 and 2000, respectively.

From 1996 to 2000, he was with the Electromagnetic Compatibility Laboratory, University of Missouri-Rolla. He then joined the Desktop Architecture Laboratory of Intel Corporation, Hillsboro, OR, as a Senior Hardware Engineer. His research interests include numerical and experimental study of electromagnetic compatibility problems in high-speed IC and PCB designs.

Todd H. Hubing (S'82–M'82–SM'93) received the B.S.E.E. degree from the Massachusetts Institute of Technology, Cambridge, MA, in 1980, the M.S.E.E. degree from Purdue University, West Lafayette, IN, in 1982, and the Ph.D. degree in electrical engineering from North Carolina State University,Raleigh, in 1988.

From 1982 to 1989, he was employed in the Electromagnetic Compatibility Laboratory, IBM Communications Products Division, in Research Triangle Park, NC. In 1989, he joined the faculty at the University of Missouri-Rolla (UMR). He is currently a Professor of Electrical and Computer Engineering and part of a team of faculty and students at UMR that are working to solve a wide range of EMC problems affecting the electronics industry. He teaches the "Grounding and Shielding" and "High-Speed Digital Design" courses at UMR.

He has been an Associate Editor of the IEEE Transactions on Electromagnetic Compatibility, the IEEE EMC Society Newsletter, and the *Journal of the Applied Computational Electromagnetics Society*. He is currently the President of the IEEE EMC Society.